

# Green Synthesis of Phyllanthus Niruri Nanoparticles for the Treatment of Sickle Cell Anemia

Miss. Dipali B. Hiwarde<sup>1</sup>, Prof. Akolkar P. B.<sup>2</sup> Anushka M. Chavan<sup>3</sup>, Rushali J. Gore.<sup>4</sup>

UG Scholars, Rashtriya College of Pharmacy, Hatnoor, Kannad, Chh. Sambhajinagar Maharashtra, India<sup>1,3,4</sup>  
Assistant Professor, Rashtriya College of Pharmacy, Hatnoor, Kannad, Chh. Sambhajinagar Maharashtra, India.<sup>2</sup>

**Abstract:** Nanotechnology is currently the most active research area in modern materials science. While numerous chemical and physical methods exist for the synthesis of nanomaterials, the green synthesis approach is increasingly prominent. Plant-mediated synthesis of nanoparticles is a green chemical technique that integrates nanotechnology with botany. This novel method of synthesis ideally occurs at ambient temperatures, neutral pH, and is cost-effective and environmentally friendly. Given this goal, various routes have been explored for synthesizing nanomaterials.

The present study aims to formulate and evaluate herbal nanoparticles derived from *Phyllanthus niruri* for the natural treatment of sickle cell anemia. Sickle cell anemia is characterized by the presence of sickle-shaped erythrocytes caused by abnormal hemoglobin production. This condition leads to clogging of capillaries and obstructs blood flow in the vessels, resulting in severe complications such as ischemia, hypoxia, and organ failure. While some drugs, such as hydroxyurea, are available for treating sickle cell anemia, they are often associated with severe adverse effects, limiting their frequent use. Therefore, this study focuses on designing herbal nanoparticles as an alternative treatment for sickle cell anemia. The plant material for this study was sourced from an authorized market, dried, and powdered for further processing.

**Keywords:** nanomaterials

## I. INTRODUCTION

### 1.1. Nanochemistry:

Nanochemistry is the combination of Chemistry and Nano science. It is associated with synthesis of building blocks which are dependent on size, surface, shape and defect properties. It is being used in chemical, materials and physical, science as well as engineering, biological and medical applications. This also involves the study of synthesis and characterization of materials of Nano scale size. It is relatively a new branch of chemistry that is concerned with unique properties associated with assemblies of atoms or molecules of nano scale size (1-100nm) so the nanoparticles lie somewhere between individual atoms or molecules of bulk materials [1]. It has uses in chemical, physical and materials science, engineering and biological and medical applications. Using single atoms as building blocks offers new ways to create innovative materials, the opportunity to create the smallest features possible in integrated circuits and the chance to explore quantum computing for example. It might seem relatively new, but nanochemistry has been employed for many years, for example in sunscreens that absorb UV light, in clear coatings for cars which protect the bright paint colours underneath, or in carbon nanotubes for lightweight car parts or sporting equipment. It has been used to study the health and safety effects of airborne and waterborne nanosized particulates, and nanoparticles have been used to clear up or neutralizes pollutants.

### 1.2 Applications of Nanochemistry

#### 1.2.1 Medicine

One highly explained application of Nano-chemistry in medicine. A simple skin-care product using the technology of Nano-chemistry is sunscreen. Sunscreen contains nanoparticles of zinc oxide and titanium dioxide. These chemicals protect the skin against harmful UV light by absorbing or reflecting the light and prevent the skin from retaining full

damage by photo excitation of electrons in the nanoparticle. Effectively, the excitation of the particle blocks skin cells from DNA damage [2].

### **1.2.2 Catalysis Nanoenzymes**

Nanostructure materials mainly used in nanoparticle-based enzymes have drawn attraction due to the specific properties they show. Very small size of these Nanoenzymes (or Nanozymes) (1–100 nm) have provided them unique optical, magnetic, electronic, and catalytic properties. Moreover, the control of surface functionality of nano particles and predictable nanostructure of these small sized enzymes have made them to create a complex structure on their surface which in turn meet the needs of specific applications [3].

### **1.2.3 Wounds**

For abrasions and wounds, Nano chemistry has demonstrated applications in improving the healing process. Electro spinning is a polymerization method used biologically in tissue engineering, but can be functionalized for wound dressing as well as drug delivery. This produces Nano fibers which encourage cell proliferation, antibacterial properties, and controlled environment. These properties have been created in macroscale; however, nanoscale versions may show improved efficiency due to nanotopographical features. [4]. Targeted interfaces between nanofibers and wounds have higher surface area interactions and are advantageously in vivo [5]. There is evidence certain nanoparticles of silver are useful to inhibit some viruses and bacteria. New developments in nanochemistry provide a variety of nanostructure materials with significant properties that are highly controllable. Some of the application of these nanostructure materials include self-assembled monolayers and lithography, use of nanowires in sensors, and nanoenzyme.

### **1.3 Green Synthesis of Nanoparticles**

Green chemistry (sustainable chemistry): Design of chemical products and processes that reduce or eliminate the use or generation of substances hazardous to humans, animals, plants, and the environment. Green chemistry discusses the engineering concept of pollution prevention and zero waste both at laboratory and industrial scales. It encourages the use of economical and Eco compatible techniques that not only improve the yield but also bring down the cost of disposal of wastes at the end of a chemical process. [6]

In materials science, “green” synthesis has gained extensive attention as a reliable, sustainable, and eco-friendly protocol for synthesizing a wide range of materials/nanomaterials including metal/metal oxides nanomaterials, hybrid materials. As such, green synthesis is regarded as an important tool to reduce the destructive effects associated with the traditional methods of synthesis for nanoparticles commonly utilized in laboratory and industry. Green syntheses are required to avoid the production of unwanted or harmful by-products through the build-up of reliable, sustainable, and eco- friendly synthesis procedures. The use of ideal solvent systems and natural resources (such as organic systems) is essential to achieve this goal. Green synthesis of metallic nanoparticles has been adopted to accommodate various biological materials (e.g., bacteria, fungi, algae, and plant extracts). Among the available green methods of synthesis for metal/metal oxide nanoparticles, utilization of plant extracts is a rather simple and easy process to produce nanoparticles at large scale. Green synthesis of nanoparticles has many potential applications in environmental and biomedical fields. The plants are considered to be more suitable compared to microbes for green synthesis of nanoparticles as they are non-pathogenic and various pathways are thoroughly researched. A wide spectrum of metal nanoparticles has been produced using different these nanoparticles have unique optical, thermal, magnetic, physical, chemical, and electrical properties [7]

**1.4 Classification of NPs:**

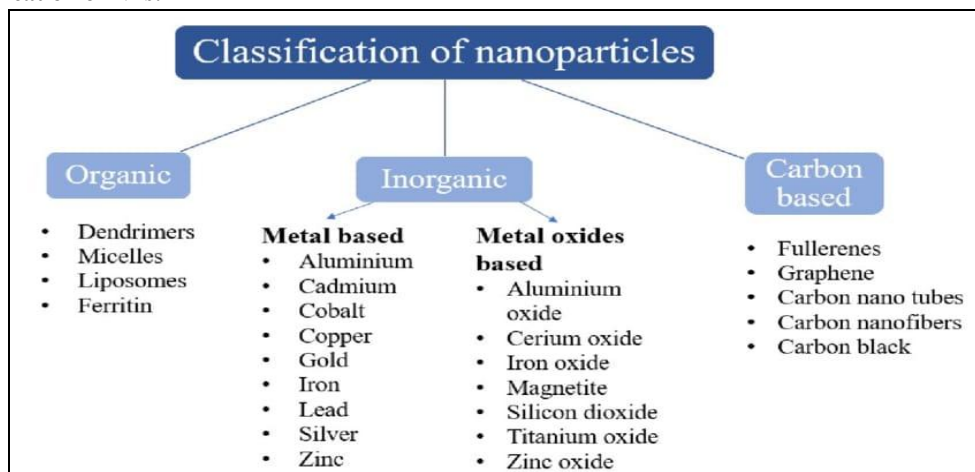


**Fig.1.1 : Classification of Nanoparticles**

**1.4. Green Synthesis of Silver Nanoparticles**

Plant extract mediated synthesis always takes place extracellularly, and the reaction times have also been reported to be very short compared to that of microbial synthesis. Most importantly, the process can be suitably scaled up for large scale synthesis of NPs.

Many plants such as *Pelargonium graveolens* [8], *Medicagosativa* [9], *Azadirachtaindica* [10], *Lemongrass* [ 11], *Aloe Vera* [12], *Cinnamomum Camphora* , *Emblicaoofficialis* , *Capsicum annum* , *Diospyros kaki* , *Carica papaya* [13], *Coriandrum* sp. [14], *Boswelliaovalifoliolata* [15], *Tridaxprocumbens*, *Jatrophacurcas*, *Sola nummelongena*, *Daturametel*, *Citrus aurantium* [16], and many weeds have shown the potential of reducing silver nitrate to give formation of AgNPs.

*Phyllanthus Niruri* is a medicinal herb abundantly found and cultured in India, Malaysia, Australia, West Africa, and some of the Arab countries [17]. *Phyllanthus Niruri* leaves have been traditionally used for treatment of many infections. The antibacterial activity has been reported to be the upshot of essential oil components, mostly eugenols found in it. *Phyllanthus Niruri* leaves have been traditionally used for treatment of many infections. The antibacterial activity has been reported to be the upshot of essential oil components, mostly eugenols found in it. The present study aims at the synthesis of silver nanoparticles from the aqueous extract of *Phyllanthus Niruri* leaves. We also attempt to combine the inherent antimicrobial activities of silver metal and *Phyllanthus niruri* extract for enhanced Antiscekling activity.



**Figure 2 : Silver nanoparticles**

### **1.5 Applications of Silver Nanoparticles**

#### **1.5.1 Nanoparticles are useful tools for various dental applications.**

Silver nanoparticles (AgNPs) are extensively used in dentistry to create various biomaterials for different dental applications, primarily due to their remarkable antimicrobial properties. The oral cavity acts as a gateway to the entire body, making its protection a significant goal in dentistry. Plaque biofilm is a major contributor to numerous dental diseases, and various biomaterials incorporating nanoparticle applications have become invaluable tools in addressing these issues in endodontics, periodontics, restorative dentistry, orthodontics, and oral cancers.

Among these biomaterials, silver nanoparticles stand out for their antimicrobial efficacy. They are incorporated into biomaterials to prevent or minimize biofilm formation due to their high surface-to-volume ratio and small particle size, enabling excellent antimicrobial action without compromising the mechanical properties of the material. This unique characteristic of AgNPs makes them preferred fillers in various biomaterials, playing a crucial role in enhancing their properties. [18]

#### **1.5.2. Silver nanoparticles are employed in cotton fabric through an antibacterial impregnation method to imbue the fabric with antibacterial properties.**

A novel nano-silver colloidal solution was prepared in one step by mixing AgNO<sub>3</sub> aqueous solution and an amino-terminated hyperbranched polymer (HBP-NH<sub>2</sub>) aqueous solution under vigorous stirring at room temperature. Cotton fabric was treated with nano-silver colloid by an impregnation method to provide the cotton fabric with antibacterial properties. The whiteness, silver content, antibacterial activity and washing durability of the silver-treated fabrics were determined. The results indicated that the silver-treated cotton fabric showed 99.01 % bacterial reduction of *Staphylococcus aureus* and 99.26 % bacterial reduction of *Escherichia coli* while the silver content on cotton was about 88 mg/kg. The antimicrobial activity of the silver-treated cotton fabric was maintained at over 98.77 % reduction level even after being exposed to 20 consecutive home laundering conditions. In addition, the results of scanning electron microscopy (SEM) and X-ray photoelectron spectroscopy (XPS) confirmed that silver nanoparticles have been fixed and well dispersed on cotton fabrics' surface and the major state of the silver presented on the surface was Ag<sup>0</sup>. [19]

#### **1.5.3 Silver nanoparticles offer promising potential in viral inhibition, representing a new frontier in antiviral research.**

Silver nanoparticles demonstrate potent antimicrobial properties compared to other salts due to their large surface area, facilitating enhanced contact with microorganisms. These nanoparticles adhere to the cell membrane and can penetrate bacteria. Inside the bacterial cell, silver nanoparticles interact with sulfur-containing proteins in the membrane and phosphorus-containing compounds like DNA. This interaction creates a low molecular weight region within the bacteria, leading to conglomerate formation. Consequently, DNA is shielded by silver ions, inhibiting replication and ultimately causing cell death by disrupting the respiratory chain and halting cell division. The antimicrobial efficacy of silver ions is further amplified when they are released from nanoparticles within the bacterial cell. [20].

#### **1.5.4. Applications of silver nanoparticles in food package.**

Silver nanoparticles (AgNPs) exhibit broad-spectrum antimicrobial activity against both pathogenic bacteria and spoilage fungi. Despite their efficacy, the precise mechanisms underlying their antimicrobial action remain partially understood. Currently, there is a growing scientific interest in the biological synthesis of AgNPs. These nanoparticles can be integrated into both biodegradable and non-biodegradable polymers to create food packaging with antimicrobial properties, thereby enhancing food safety and extending shelf life. Nevertheless, it is crucial to conduct migration tests on new food packaging materials containing AgNPs to determine the appropriate levels for their incorporation. [21].

### **1.6 Sickle Cell Anemia**

Sickle cell disease is an inherited autosomal recessive disorder of the  $\beta$ -globin gene characterized by clinical manifestations such as hemolytic anemia and recurrent episodes of vascular occlusion.[22] Sickle cell disease encompasses a group of inherited disorders affecting red blood cells, with sickle cell anemia being one of the primary conditions. The presentation and progression of sickle cell anemia can vary greatly among individuals. These variations in clinical manifestations are thought to be influenced by environmental factors, the degree of red blood cell

sickling, as well as the involvement of the vascular endothelium, platelets, leukocytes, and plasma proteins.[23]

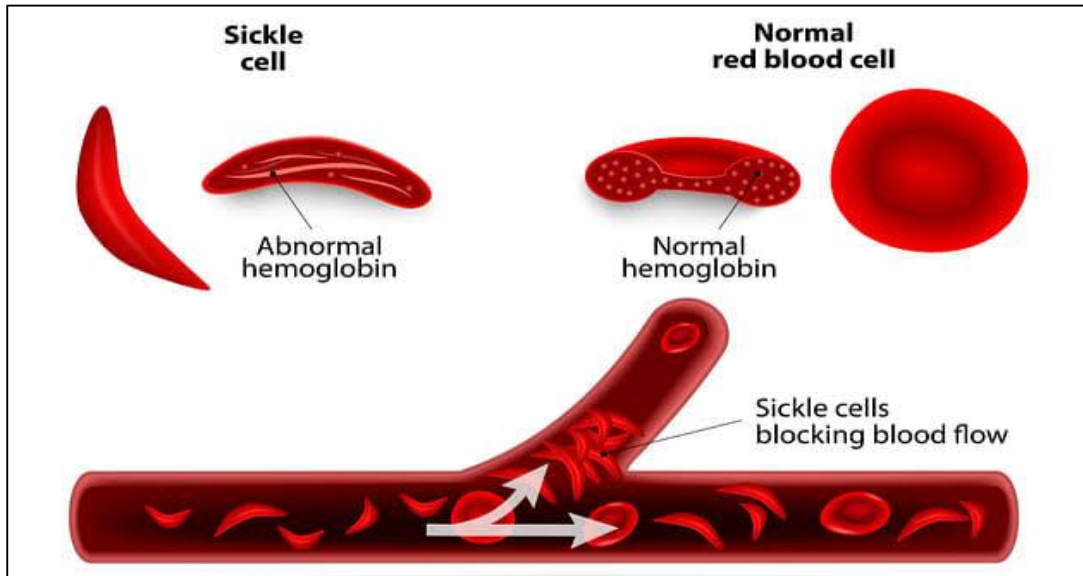


Figure No.3 : Sickle cell vs normal cell

While sickle cell disease is found globally, its prevalence is highest in sub-Saharan Africa.[24] The disease is caused by a mutation in the  $\beta$ -globin gene on chromosome 11, specifically at the 17<sup>th</sup> nucleotide, where adenine is substituted for thymine. This mutation results in the replacement of glutamic acid with valine during protein translation, producing abnormal hemoglobin. This abnormal hemoglobin is insoluble and tends to polymerize under conditions of reduced oxygen tension, trauma, stress, dehydration, acidosis, or exposure to cold environments.[25] Polymerised haemoglobin produces rigid, less flexible, and fragile erythrocytes with a reduced life span. These changes lead to various acute and chronic complications. [26].The clinical manifestations of sickle cell disease can vary widely among patients. Some common presentations include leg ulcers, priapism, fatigue, dizziness, osteonecrosis, bacteremia, and dactylitis. Other complications may involve renal disease, pulmonary hypertension, acute chest syndrome, and end-organ damage. [27] The World Health Organization (WHO) recognizes sickle cell disorder as a condition with significant global impact, particularly noting its substantial public health implications for Africa.[28]

According to available data, approximately 4.4 million individuals worldwide are affected by sickle cell disease, whereas around 43 million people are carriers of the sickle cell trait.[29] About 80% of sickle cell disease cases occur in sub-Saharan Africa,[8] and the mortality rate for children under the age of 5 with sickle cell disease ranges from 50% to 80%. This high burden of the disease is worsened by limited access to comprehensive healthcare services in the region.[30]

Africa has been associated with the highest prevalence of the sickle cell trait, with figures suggesting that between 10% and 40% of the entire population may be affected.[31] The prevalence of sickle cell trait varies across different countries in Africa, with incidence rates ranging from 20% to 30% in countries like Cameroon, the Democratic Republic of the Congo, Gabon, Ghana, and Nigeria. In certain regions of Uganda, a particularly high prevalence of 45% has been reported.[32] The data indicates that approximately 90% of the global sickle cell disease population resides in Nigeria, India, and the Democratic Republic of the Congo, where the disease affects up to 2% of the population.[33] Evidence suggests Nigeria has the largest population of persons affected with sickle cell disease globally.[34,35]

Considering the significant burden of sickle cell disease in sub-Saharan Africa and the insufficient measures to manage related crises, there is surprisingly limited evidence in the existing literature that thoroughly analyzes emerging issues associated with the disease. This study aims to critically review research focusing on the challenges of sickle cell disease in sub-Saharan Africa. Considering the significant burden of sickle cell disease in sub-Saharan Africa and the insufficient measures to manage related crises, there is surprisingly limited evidence in the existing literature that

thoroughly analyzes emerging issues associated with the disease. This study aims to critically review research focusing on the challenges of sickle cell disease in sub-Saharan Africa.

### 1.7 Phyllanthus Niruri:

#### 1.7.1 Herbal Plant Profile:

Taxonomical Classification of Phyllanthus Niruri – There are botanical classification of Phyllanthus Niruri.

Kingdom	Plantae
Division	Tracheophyta
Class	Magnoliopsida
Order	Malpighiales
Family	Phyllanthaceae
Genus	Phyllanthus
Species	Phyllanthus Niruri

Table 1. Taxonomical Classification of Phyllanthus Niruri

Languages	Vernacular Names of Bhumi Amla
Common name	Phyllanthus, Stonebreaker, gale of wind
Sanskrit name	BahuPatra, Tamalaki, Bahuphala
Hindi name	Bhumi amla, Jangli Amlai
Marathi	Bhui avla, Bhui amla
Kannada	Bhu nelli, Nelanelli
Tamil	Kilanelli
Telugu	Nela usiraka
Urdu	Bhumi Amla
Spanish	Chanca Piedra

Table 2. Vernacular Names of Bhumi Amla[36]

Plant Parts Used – The following parts of Phyllanthus Niruri are used –

Leaves, stems, seeds, fruits, and whole plants.[37]

#### 1.7.2 Morphology of Phyllanthus Niruri –

Phyllanthus Niruri is a weed that grows around 50 – 70 c.m. high and bears ascending herbaceous branches.

Leaves – Leaves of Phyllanthus Niruri are alternate in small size and arranged in two rows. These are small, numerous green, sub sessile, closely arranged having short petiole and stipules present, they are arranged alternatively on each side of the stem.



Figure No. 4 – Leaves of the Phyllanthus Niruri

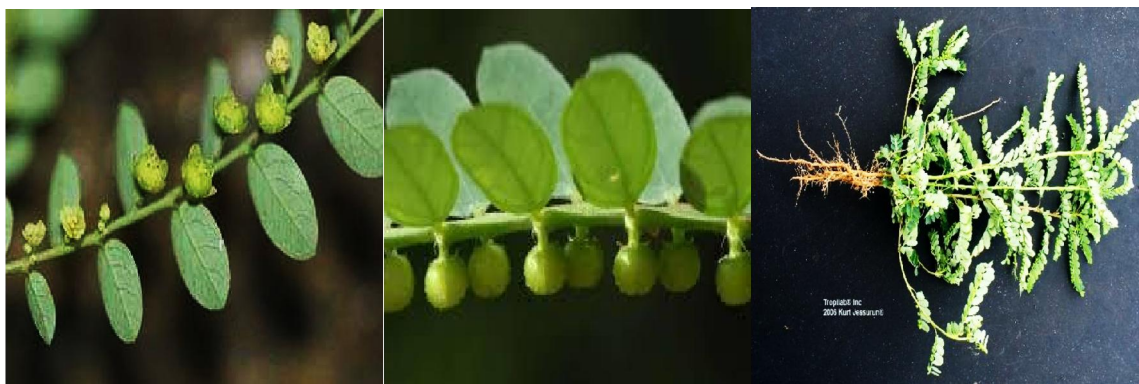
Flowers – Phyllanthus Niruri bears unisexual, monoecious flowers. The female flowers are solitary, while the male flowers have 1-3 sessile stamens. The bark of the plant is smooth and light green, and it produces numerous pale green flowers. These flowers are small, axillary, and yellowish in color.

Fruits – The fruit of Phyllanthus Niruri is a very small, depressed globose capsule. These capsules are smooth, approximately 2-3 mm in diameter, and each branch of the plant bears fruit on the back of the leaf. These fruit capsules resemble small, smooth capsules filled with seeds.

Stem – The stem of Phyllanthus Niruri features horizontal branches and is typically 1-2.5 mm in width. The stem itself ranges in height from 30 to 60 cm.

Root – Roots of this plant branched and large.

Phyllanthus Niruri is commonly found in temperate climates across coastal regions of India. It typically produces flowers and fruits during the rainy season, with flowers appearing first, followed by fruits later in the season.



Phyllanthus Niruri is commonly found in temperate climates across coastal regions of India. It typically produces flowers and fruits during the rainy season, with flowers appearing first, followed by fruits later in the season.[38]

1.7.3 Chemical Constituents of Phyllanthus Niruri –Based on the physical and chemical properties of herbs, five compounds have been isolated from different parts of Phyllanthus Niruri.[10] These compounds include (1) Corilagin, (2) Ruffin, (3) Isobubbialine, (4) Succinic acid, and (5) Gallic acid. Phyllanthus niruri is a medicinal plant known for its diverse range of phytochemicals and pharmacological properties. The chemical constituents that have been isolated from various parts of Phyllanthus niruri include flavonoids, terpenoids, lignans, alkaloids, tannins, polyphenols, coumarins, and saponins. These herbal extracts have demonstrated clinical effects in research studies.[39]

Leaf:

1. 4-Hydroxy-lintetralin, Lf.
2. 2,3-Dimethoxy-isolintertralin, Lf
3. Astragalin, Lf
4. Beta-sitosterol, Lf
5. Demethylenedioxy niranthin, Lf.
6. Hydroxy niranthin, Lf
7. Hypophyllanthin, Lf Aer

Root –

1. (+)-Catechin, Rt cult
2. (+) Gallocatechin, Rt Cult
3. (-) Epicate chin, Rt Cult
4. (-) Epicate chin-3gallate, Rt Cult
5. (-) Epigalloca techin, Rt Cult
6. Gallic acid, Rt cult
7. Epigalloca techin-3-Ogalla te, Rt

8. Eriodictyol-7-o-alpha-L-rhamnoside, Rt
9. Fisetin-41-O-alpha-L-rhamnoside, Rt
10. Lupeol acetate, Rt
11. Lupeol, Rt
12. Nor-securinine, Rt.
8. Iso-quercetin, Lf
9. Linnanthin, Lf
10. Lintetralin, Lf
11. Niranthin, Lf
12. Quercitrin, Lf
13. Salicylic acid methyl ester, Lf EO
14. Seco-4-hydroxy-lintetralin.

**Aerial Parts –**

- 1.24-Isopropyl Cholestrol, Aer
2. Dotriacontanoic acid, Aer
3. Nirphyllin, Aer
4. Nirurine, Aer
5. Phyllanthenol, Aer
6. Phyllantheol, Aer
7. Phyllester, Aer
8. Phyllinurin, Aer
9. Phylltetrin, Aer
10. Triacontan-1-al, Aer
11. Triacontan-1ol, Aer.

**Leaf, Stem –**

1. Nirtetralin, Pl, Lf
2. 4-Methoxy-nor securinine, Aer, Rt, St
3. Rutin, Pl, Lf
4. Phyllanthine, Rt, Lf, St
5. Phyllochrysine, Lf, St
6. Quercetin, Lf, Pl

**Essential Oil –**

1. Kaempferol-4-o-alpha-L-rhamnoside, Aer 0.9%, Rt,
2. (-) Limonine, Lf EO 4.5%,
3. Ascorbic acid, Lf 0.41%,
4. Cymene, Lf EO 11%,
5. Hypophyllanthin, Pl 0.05-0.17%,
6. Geranin, Pl .23%,7
7. Linoleic acid, Sd Ol 21%,
8. Linolenic acid, Sd Ol 51.4%,



9. Ricinoleic acid, Sd Ol 1.2%,
10. Phyltetralin, Pl, Lf 0.14% and
11. Phyllanthin, Lf, Aer.

### 1.8 Characterization Techniques

Characterization, when used in material science, refers to the use of external techniques to probe into the internal structure and properties of a material. Characterization can take the form of actual materials testing or analysis. Analysis techniques are used to simplify to magnify the specimen, to visualise its internal structure, and to gain knowledge as to the distribution of elements within the specimen and their interactions.

#### 1.8.1 X-RAY DIFFRACTION ANALYSIS:

The Definition of x-ray diffraction is: Diffraction of light means the bending of light around the corner of an obstacle. It is a fact that for diffraction to occur. The size of the obstacle should nearly be equal to the wavelength of light used. X-ray, like other electromagnetic rays, can also be diffracted, but for the diffraction of X-ray. The size of the obstacle should be a few angstroms (approx 1 Å) which is approximately the wavelength of X rays. Since the atomic spacing in the Crystal is nearly a few Å.

X-ray diffraction is based on constructive interference of monochromatic X- rays and a crystalline sample. These X-rays are generated by a cathode ray tube, filtered to produce monochromatic radiation, collimated to concentrate, and directed toward the sample. When a monochromatic x-ray incident occurs on a crystal. The atomic electrons in the Crystal are sent into vibration. With the same frequency as that of the frequency of the incident ray and are accelerated. These Accelerated electrons then emit the radiation of the same frequency as that of incident x-rays in all directions. If the wavelength of incident radiation is large compared to the dimensions of the Crystal. Then the radiated X-ray are in phase with each. But since the atomic dimension are nearly equal to the wavelength of X-Ray. The radiation emitted by the electrons is out of phase with each other. These radiations may interfere constructively or destructively producing a diffraction pattern (i.e. maxima and minima) in certain directions.

Bragg's Law of Diffraction:

In order to explain the diffraction of x rays, W.L. Bragg considered the X-ray diffraction from a crystal as a problem of reflection of X-rays from the atomic planes of the crystal in accordance with the laws of reflection. Consider a set of parallel atomic planes of the Crystal with Miller Indices [hkl], such that the distance between the two successive planes is  $d$ . Let a parallel beam of monochromatic X-rays of wavelength  $\lambda$  be incident on the Plane at a glancing angle  $\theta$  such that the incident rays lie in the plane of the paper.

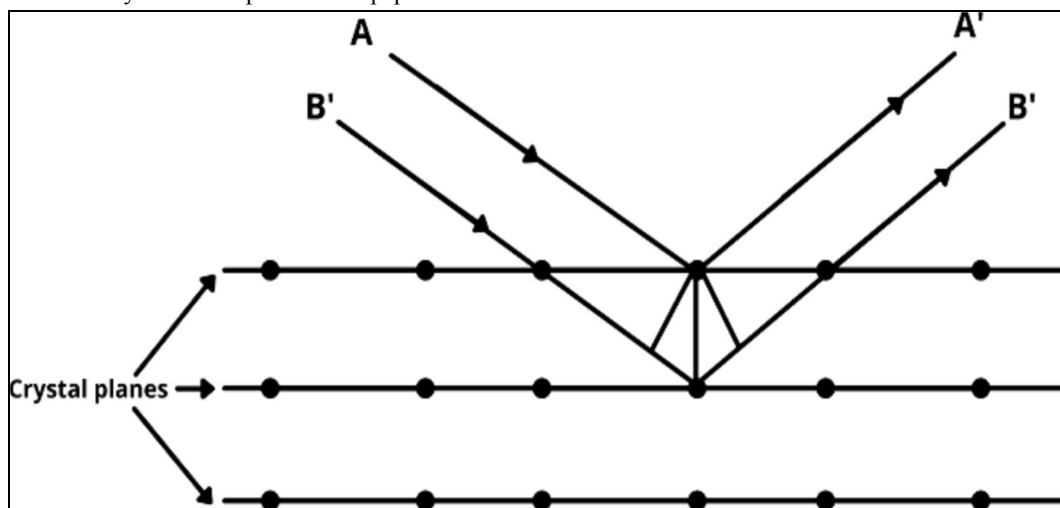


Figure No. 6 : XRD

Let AP and BQ be two parallel incident rays that are reflected from points P and Q on the Crystal planes and travel along with PA' and QB' respectively. If the path difference between APA' and BQB' is an integral multiple of  $\lambda$ , there will be constructive interference and a maximum will be observed [40].

### 1.8.2 FTIR SPECTROSCOPY

Fourier transform infrared spectrometer (FTIR) is one of the instruments based on infrared spectroscopy. It is the most modern type and preferred over the other dispersive spectrometers. It is because of its high precision, accuracy, speed, enhanced sensitivity, ease of operation, and sample non destructiveness. The fundamental of infrared spectroscopic technology is on atomic vibrations of a molecule that only absorbs specific frequencies and energies of infrared radiation. The molecules could be detected and classified by FTIR because different molecules will have different infrared spectrum. A block diagram of FTIR working process is shown in Figure 3. The FTIR spectrometer essentially uses an interferometer to measure the energy that is being transmitted to the sample. The infrared radiation emitted from the black body reaches the interferometer where the spectral encoding of signals happens. The resultant interferogram signal is transmitted through or bounces from the sample surface, where specific energy wavelengths are absorbed. The beam eventually passes through the detector and further passed on to processing computer for Fourier transformation of energy signals [41]

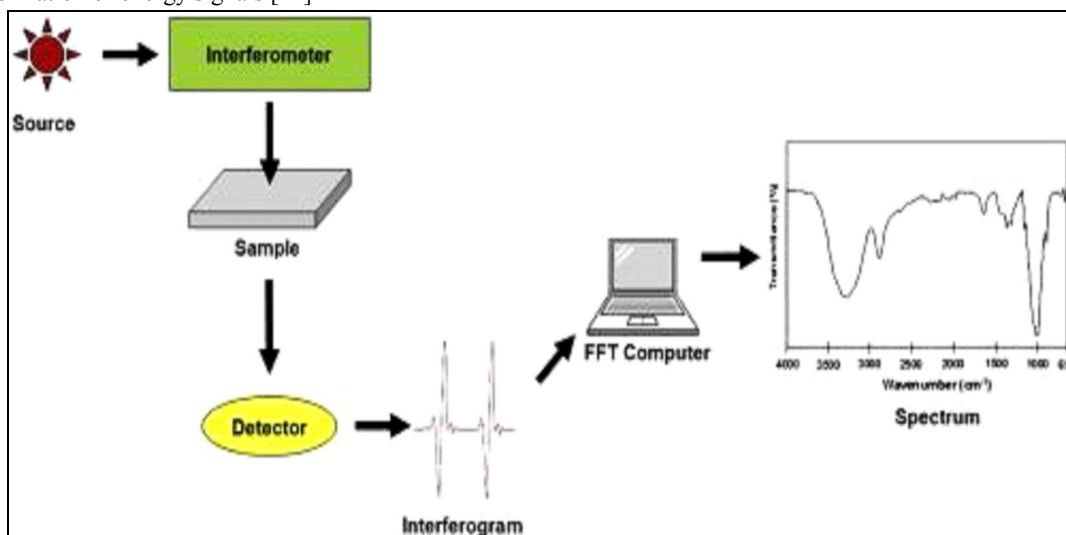


Figure No. 7: FTIR block diagram

### 1.8.3 SCANNING ELECTRON MICROSCOPE :

A scanning electron microscope (SEM) is a type of electron microscope that produces images of a sample by scanning the surface with a focused beam of electrons. The electrons interact with atoms in the sample, producing various signals that contain information about the surface topography and composition of the sample. The electron beam is scanned in a raster scan pattern, and the position of the beam is combined with the intensity of the detected signal to produce an image. In the most common SEM mode, secondary electrons emitted by atoms excited by the electron beam are detected using a secondary electron detector (Everhart-Thornley detector). The number of secondary electrons that can be detected, and thus the signal intensity, depends, among other things, on specimen topography. Some SEMs can achieve resolutions better than 1 Nanometre. Specimens are observed in high vacuum in a conventional SEM, or in low vacuum or wet conditions in a variable pressure or environmental SEM, and at a wide range of cryogenic or elevated temperatures with specialized instruments [42]. The signals used by an SEM to produce an image result from interactions of the electron beam with atoms at various depths within the sample

Various types of signals are produced including secondary electrons (SE), reflected or back-scattered electrons (BSE), characteristic X-rays and light (cathodoluminescence) (CL), absorbed current (specimen current) and transmitted electrons. Secondary electron detectors are standard equipment in all SEMs, but it is rare for a single machine to have

detectors for all other possible signals. Secondary electrons have very low energies on the order of 50 eV, which limits their mean free path in solid matter. Consequently, SEs can only escape from the top few nanometers of the surface of a sample. The signal from secondary electrons tends to be highly localized at the point of impact of the primary electron beam, making it possible to collect images of the sample surface with a resolution of below 1 nm. Back-scattered electrons (BSE) are beam electrons that are reflected from the sample by elastic scattering. Since they have much higher energy than SEs, they emerge from deeper locations within the specimen and, consequently, the resolution of BSE images is less than SE images. However, BSE are often used in analytical SEM, along with the spectra made from the characteristic X-rays, because the intensity of the BSE signal is strongly related to the atomic number (Z) of the specimen. BSE images can provide information about the distribution, but not the identity, of different elements in the sample. In samples predominantly composed of light elements, such as biological specimens, BSE imaging can image colloidal gold immune-labels of 5 or 10 nm diameter, which would otherwise be difficult or impossible to detect in secondary electron images [43].

Characteristic X-rays are emitted when the electron beam removes an inner shell electron from the sample, causing a higher-energy electron to fill the shell and release energy. The energy or wavelength of these characteristic X-rays can be measured by Energy-dispersive X-ray spectroscopy or Wavelength-dispersive X-ray spectroscopy and used to identify and measure the abundance of elements in the sample and map their distribution. Due to the very narrow electron beam, SEM micrographs have a large depth of field yielding a characteristic three-dimensional appearance useful for understanding the surface structure of a sample [44]. This is exemplified by the micrograph of pollen shown above. A wide range of magnifications is possible, from about 10 times (about equivalent to that of a powerful hand-lens) to more than 500,000 times, about 250 times the magnification limit of the best light microscopes.

#### **1.8.4 SYNTHESIS OF SILVER NANOPARTICLES:**

In recent years silver nanoparticles have been investigated by many research groups nationally and internationally. It is mainly because of the potential application of nanoparticles in biology, medicine, optics and in modern electronic devices. Silver nanoparticles have advantage over other noble nanoparticles (e.g., gold and copper) Silver nanoparticles exhibit very strong bactericidal activity against gram-positive as well as gram negative bacteria including multi-resistant strains, as well as potential antifungal agent. In recent years silver nanoparticles have been investigated by many research groups nationally and internationally. It is mainly because of the potential application of nanoparticles in biology, medicine, optics and in modern electronic devices. Silver nanoparticles have advantage over other noble nanoparticles (e.g., gold and copper) Silver nanoparticles exhibit very strong bactericidal activity against gram-positive as well as gram negative bacteria including multi-resistant strains, as well as potential antifungal agent.

## **II. MATERIAL AND METHOD:**

### **2.1 Synthesis Of Silver Nanoparticles**

In recent years, research groups both nationally and internationally have extensively investigated silver nanoparticles. This interest is primarily driven by their potential applications in biology, medicine, optics, and modern electronic devices. Silver nanoparticles offer advantages over other noble nanoparticles, such as gold and copper. They exhibit strong bactericidal activity against both gram-positive and gram-negative bacteria, including multi-resistant strains, and also hold promise as antifungal agents.

#### **Material Required:**

*Plant Sample:* : *Phyllanthus Niruri*  
*Kingdom:* *plantae-plant*  
*Subkingdom:* *Tracheobionta – Vascular plant*  
*Super division:* *Spermatophyta - Seed plant*  
*Division:* *Magnoliophyta – Flowering plants*  
*Class:* *Magnoliopsida dicotyledons*  
*Subclass:* *Rosidae*  
*Order:* *Euphorbiales*  
*Family:* *Phyllanthaceae*

Genus: *Phyllanthus L.*  
Species: *Phyllanthus Niruri L. – Gale of the wind*  
Chemicals required: 1 Molar Silver nitrate (AgNO<sub>3</sub>)

### 2.1.1 Procedure:

#### Preparation of plant extract

Healthy plant samples were collected and thoroughly cleaned using running tap water. The samples were then allowed to dry at room temperature. Approximately 40 grams of plant leaves were weighed and cut into small pieces. These finely cut pieces were mixed with 200 ml of distilled water and the mixture was boiled for 30 minutes. Once cooled to room temperature, the mixture was filtered using Whatman No. 40 filter paper.

#### Synthesis of Silver Nanoparticle

100 ml of the plant extract aqueous solution was combined with 50 ml of a 1 molar silver nitrate solution. The mixture was allowed to react at room temperature, resulting in the formation of silver nanoparticles, which were then allowed to settle. The solution was subsequently filtered using Whatman No. 40 filter paper and the nanoparticles were dried.

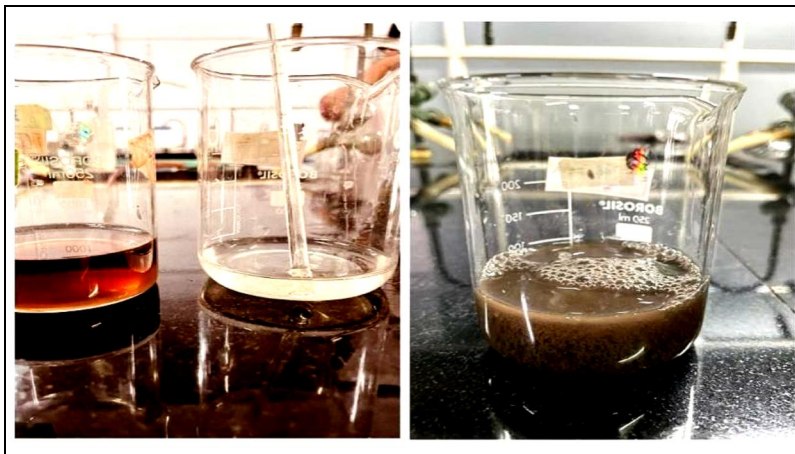


Figure No. 8: Preparation of silver nanoparticles

## III. RESULTS AND DISCUSSION

This chapter gives brief description of the experimental results obtained after doing the analysis - XRD, FTIR and SEM.

### 3.1 X-Ray Diffraction Studies- Silver Nanoparticles

The XRD pattern of the silver nanoparticles is.

From this study, considering the peak at degrees, average particle size has been estimated by using Debye-Scherrer formula,

$$D = 0.9\lambda / B \cos\theta$$

where  $\lambda$  is the wave length of X-ray (0.1541nm), B is FWHM (full width at half maximum),  $\theta$  is the diffraction angle and D is the particle diameter size and 'n' is the order of reflection. The calculated particle size details are in table.

Calculations- Particle size determination by XRD

1. Silver nanoparticles prepared from Phyllanthus Niruri.

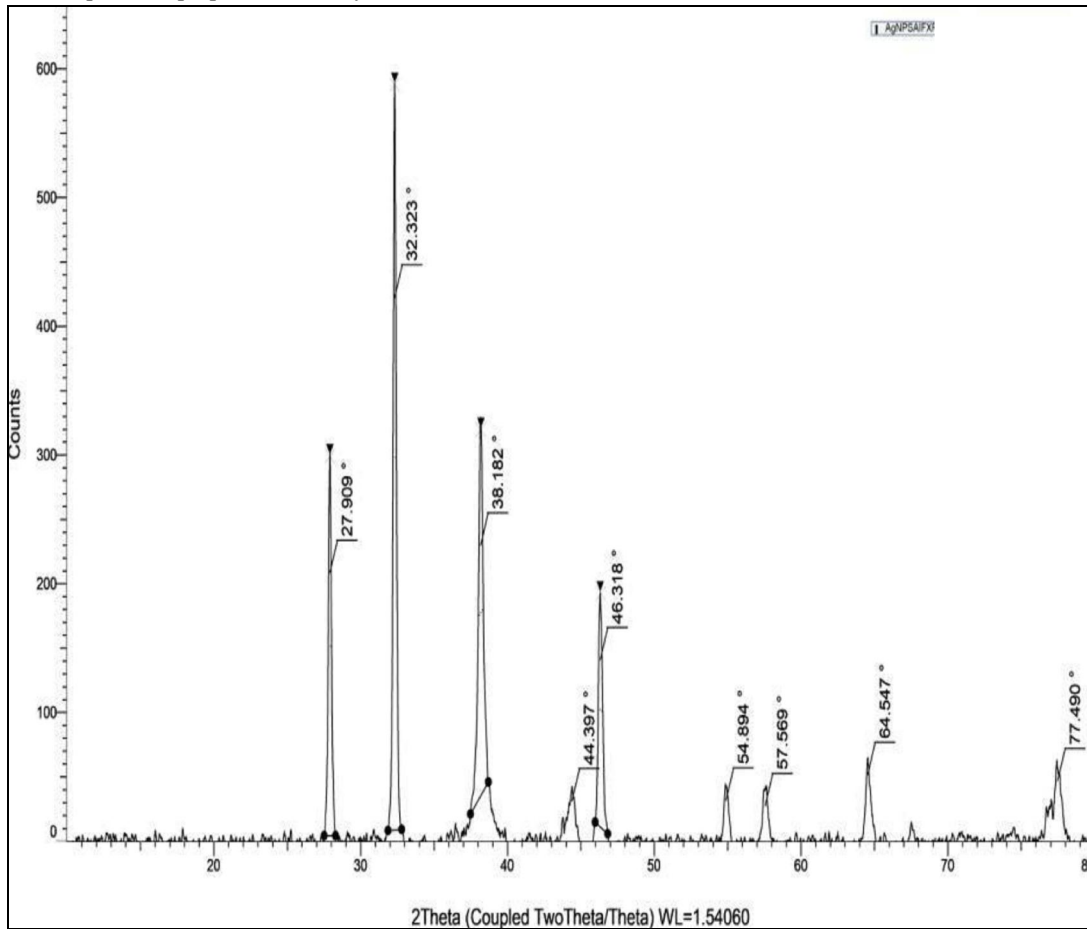


Figure No. 9 : X-RAY DIFFRACTION STUDIES- SILVER NANOPARTICLES

Peak-1:-

$$2\theta = 27.910^\circ$$

$$\theta = 13.955^\circ = 0.2434 \text{ radian } B = 0.224 = 0.003909 \text{ radian}$$

$$\lambda = 1.5406 \times 10^{-10} \text{ m}$$

From Debye-scherrer equation,

$$D = 0.9\lambda / B \cos\theta = 0.9 \times 1.5406 \times 10^{-10} / 0.003909 \times \cos(0.2434) = 35.4707 \text{ nm}$$

Peak-2:-

$$2\theta = 32.329^\circ$$

$$\theta = 16.1645^\circ = 0.28198 \text{ radian } B = 0.227 = 0.003962 \text{ radian}$$

$$\lambda = 1.5406 \times 10^{-10} \text{ m}$$

From Debye-scherrer equation,

$$D = 0.9\lambda / B \cos\theta = 0.9 \times 1.5406 \times 10^{-10} / 0.003962 \times \cos(0.28198) = 34.9963 \text{ nm}$$

Peak-3:-

$$2\theta = 38.188^\circ$$

$$\theta = 19.094^\circ = 0.3330 \text{ radian } B = 0.345 = 0.006021 \text{ radian}$$

$$\lambda = 1.5406 \times 10^{-10} \text{ m}$$

From Debye-scherrer equation,

$$D = 0.9\lambda / B \cos\theta = 0.9 \times 1.5406 \times 10^{-10} / 0.006021 \times \cos(0.3330) = 23.0287 \text{ nm}$$

Peak-4:-

$$2\theta = 46.345^\circ$$

$$\theta = 23.1725^\circ = 0.4044 \text{ radian } B = 0.314 = 0.00548 \text{ radian}$$

$$\lambda = 1.5406 \times 10^{-10} \text{ m}$$

From Debye-scherrer equation,

$$D = 0.9\lambda / B \cos\theta = 0.9 \times 1.5406 \times 10^{-10} / 0.00548 \times \cos(0.4044) = 25.3024 \text{ nm}$$

$$\text{Mean value} = (35.4707 + 34.9963 + 23.0287 + 25.3024) / 4 = 29.6995 \text{ nm}$$

2 $\theta$ of the intense peak	FWHM Of intense peak	Size of the particle (D) nm	Average particle size(nm)
27.910 $^\circ$	0.003909	35.4707	29.6995
32.329 $^\circ$	0.003962	34.9963	
38.188 $^\circ$	0.006021	23.0287	
46.3450	0.00548	25.3024	

**Table 3 : Average particle size of AgNP**

The X-ray diffraction pattern of the silver nanoparticles is shown in Fig.8. The diffraction peaks are sharp which indicate that the crystalline nature is present. The size of the silver nanoparticles estimated from Debye– Scherer formula (Instrumental broadening) is 29.6995nm

### 3.2 FTIR RESULT ANALYSIS:

FT-IR analysis: FTIR spectroscopy was employed to characterize the different functional groups of the samples of AgNP. The spectrum was recorded in the range of 4500-500cm<sup>-1</sup>.

The absorption peak at 3431.52cm<sup>-1</sup> is assigned to O-H stretch of alcohols and phenolic compounds of the leaf extract.

The band at 2860.03cm<sup>-1</sup> is attributed to C-H stretching of vibrations of methyl, methylene, and methoxy groups.

The absorption band at 1626.17cm<sup>-1</sup> may be due to C=N bending in amide group or C=O stretching in carboxyl group.

The absorption band at 1626.17cm<sup>-1</sup> is close to that reported for native proteins, which suggests that proteins acted as reducing and capping agents for the biosynthesis of AgNP.

The band at 1384.13cm<sup>-1</sup> corresponds to C-O-C stretching mode of alcohols and carboxylic acids.

The peak at 1049.14cm<sup>-1</sup> was assigned to the stretch of the C-O bond.

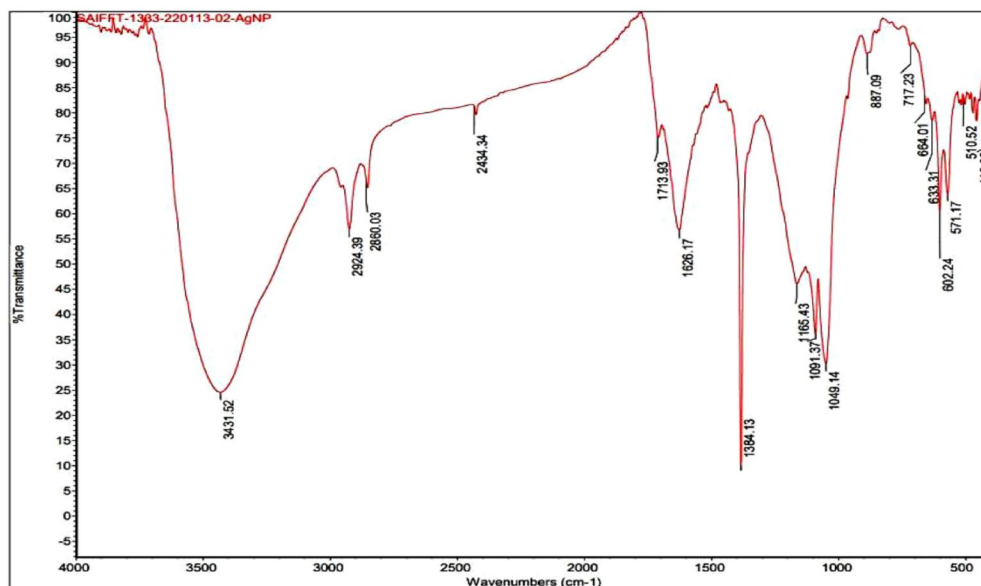


**Figure No. 10 : FTIR spectrum of AgNP**

### 3.3 pH

In present study the synthesis of silver nano-particles is faster under alkaline conditions as compared to acidic the synthesis of silver nano-particles increased as the pH towards the alkaline area where it reaches the maximum at pH 10 the appearance of the level absorption ranges at pH 4 and 6 indicates that there was no synthesis of SNPs due to they damaged by the acidity Also in the acidic milieu the biosynthesis take a longer time to change from yellow to dark brown. Moreover high PH leads to make the nanoparticles to be tend to fusion resulting the aggregation of these particles. The highest peak was 425 at pH 10 alkaline pH condition facilitated the reduction and stabilizing capacity of nitrate reductase enzyme, catalyzing the synthesis which probably activated and become more alkaline and this may be the reason for increase synthesis of AgNPs and elevation of absorbance that observed at higher pH value. High PH leads to make the nanoparticles to be tend to fusion resulting the aggregation of these particles.

### 3.4 UV- Visible spectrometry:

UV-Vis spectrophotometric analysis was carried out for the primary investigation of silver nanoparticle synthesis. A color change has been observed in the mixture of plant extract and AgNPs. The absorbance of the solution was investigated for one week.

From the spectral analysis, it is observed that the AgNPs peak was obtained at 417 nm with the highest peak and was stable thereafter for a few days as there was no increase in the absorption.

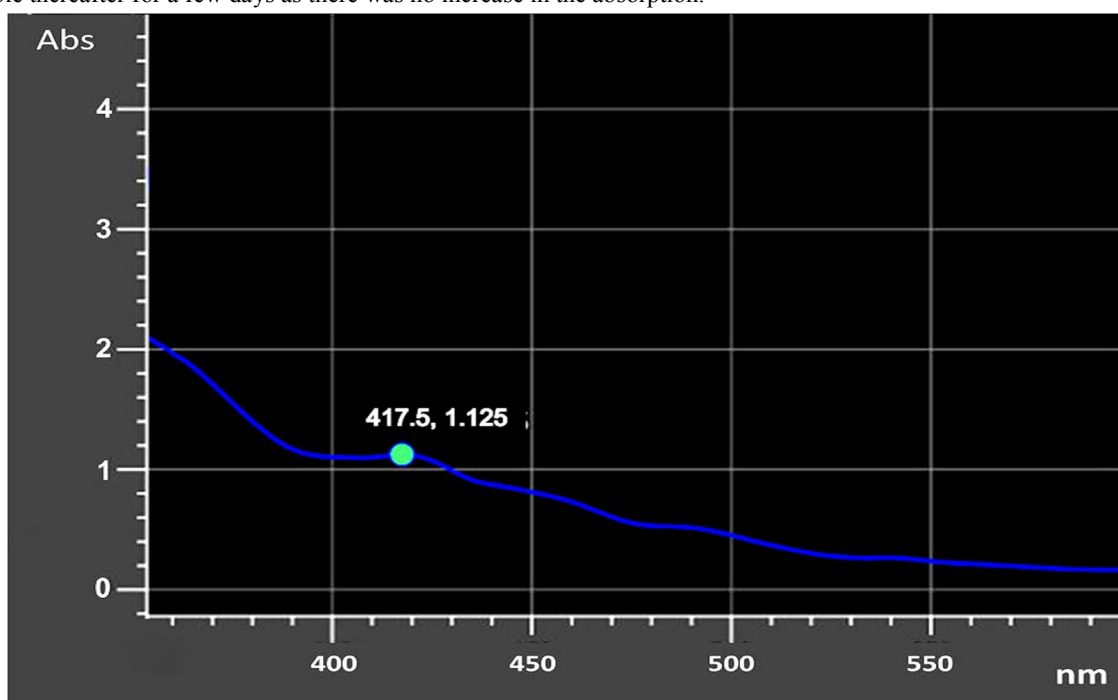


Figure No. 11: UV- Visible spectrometry analysis of biosynthesized silver nano-particles

### 3.5 SEM Analysis

The surface morphology of AgNP, were analyzed using SEM analysis. The SEM image of silver nanoparticles shows that the nanoparticles are like crystal flakes in shape and the SEM image of nHA how's that the particles are agglomerates of irregular shape, which have a tendency of leaving pores in between, the formation of pores are advantages since the permit tissue growth on implants inside the body when it is used as a biomaterial..

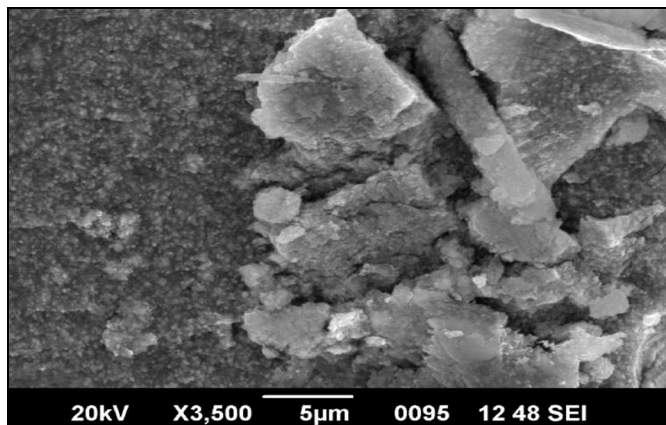


Figure No, 12: SEM image of AgNP

### 3.6 Characterization by Zeta sizer.

The surface potential of nanoparticles is the potential difference between the medium where nanoparticles are dispersed and the accessible surface of dispersed nanoparticles, which can be analyzed using a zeta sizer. Figure 4 demonstrates the zeta potential of the biosynthesized AgNPs which was found to be  $-37.8$  mV. This shows that the AgNPs synthesized from the leaf extract of *Phyllanthus Niruri* are highly stable.

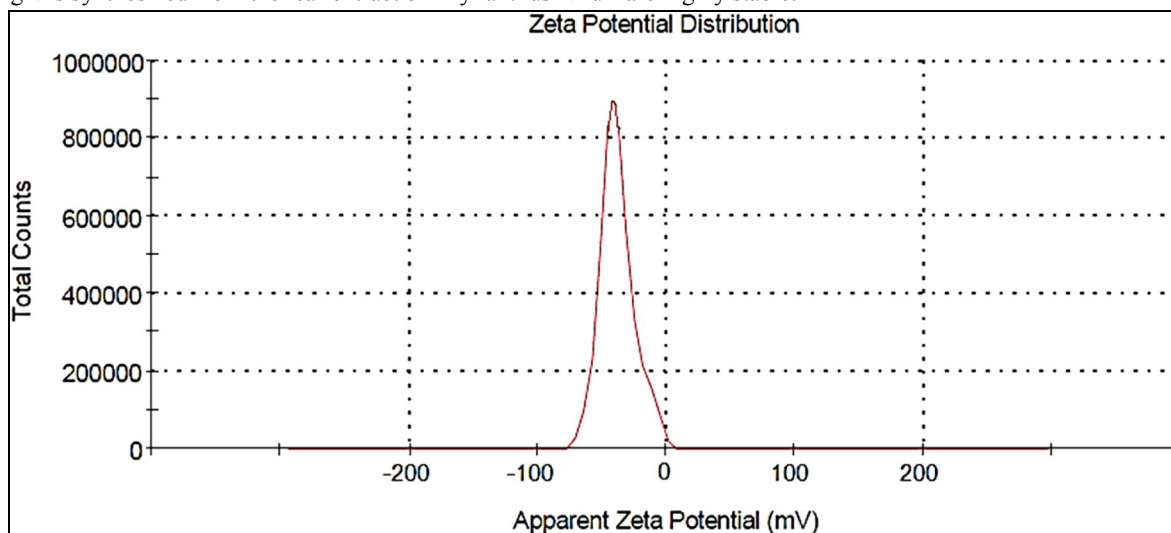


Figure No. 2.3; Zeta potential of synthesized AgNPs.

### 3.7 Temperature:

The temperature could play important role in particle formation, shape and size especially for silver nanoparticles therefore in this study, Various temperatures degree were used ( $30^{\circ}\text{C}$ ,  $60^{\circ}\text{C}$ ,  $90^{\circ}\text{C}$ ) to reach the optimum forms of nanoparticles. During color change and measurements of absorption by UV radiation with peak at  $423$  nm the results showed that the optimum temperature for the biological reduction of Ag was  $90^{\circ}\text{C}$ . This temperature ( $90^{\circ}\text{C}$ ) allowed the particles to be created at a faster rate. This result clarify the effect of temperature on the biosynthesis of nanoparticles. Most reports revealed that the reaction temperature affects the size of the nano-particles, as the temperature increases the particles size becomes smaller, An increase in the size of nanoparticles when the reaction temperature is low, while an increase in temperature reduces the size of nanoparticles.



### 3.9 pH

In present study the synthesis of silver nano-particles is faster under alkaline conditions as compared to acidic the synthesis of silver nano-particles increased as the pH towards the alkaline area where it reaches the maximum at pH 10 the appearance of the level absorption ranges at pH 4 and 6 indicates that there was no synthesis of SNPs due to they damaged by the acidity Also in the acidic milieu the biosynthesis take a longer time to change from yellow to dark brown. Moreover high PH leads to make the nanoparticles to be tend to fusion resulting the aggregation of these particles. The highest peak was 425 at pH 10 alkaline pH condition facilitated the reduction and stabilizing capacity of nitrate reductase enzyme, catalyzing the synthesis which probably activated and become more alkaline and this may be the reason for increase synthesis of AgNPs and elevation of absorbance that observed at higher pH values.

## IV. CONCLUSION

The study focused on the synthesis and characterization of silver nanoparticles (AgNPs) using Phyllanthus Niruri leaf extract. Several characterization techniques were employed, including X-ray diffraction (XRD), Fourier-transform infrared spectroscopy (FTIR), pH measurements, UV-Visible spectrometry, Scanning Electron Microscopy (SEM), Zeta potential analysis, and temperature variation studies. The key findings and conclusions are as follows:

### 1. X-ray Diffraction (XRD) Analysis

- The XRD pattern indicated that the synthesized AgNPs were crystalline in nature.
- The average particle size of AgNPs was calculated using the Debye-Scherrer formula. The mean particle size was found to be approximately 29.70 nm, with individual particle sizes ranging from 23.03 nm to 35.47 nm.

### 2. FTIR Analysis

- FTIR spectra revealed the presence of various functional groups, including O-H, C-H, C=N, C=O, and C-O-C, suggesting that proteins and other organic molecules in the leaf extract acted as reducing and capping agents during nanoparticle synthesis.

### 3. pH Influence

- The synthesis of AgNPs was more efficient under alkaline conditions, with the optimum pH being 10. Alkaline conditions facilitated the reduction and stabilization process, resulting in a higher yield of AgNPs.

### 4. UV-Visible Spectrometry

- The characteristic absorption peak of AgNPs was observed at 417 nm. This peak remained stable over several days, indicating the stability of the synthesized nanoparticles.

### 5. SEM Analysis

- SEM images revealed that the AgNPs had a crystal flake-like morphology. The presence of pores between agglomerates suggested potential applications in tissue growth on implants.

### 6. Zeta Potential Analysis

- The zeta potential of the synthesized AgNPs was measured to be -37.8 mV, indicating high stability of the nanoparticles in dispersion.

### 7. Temperature Influence

- The optimal temperature for the biological reduction of silver was found to be 90°C. Higher temperatures accelerated the formation rate and resulted in smaller nanoparticles, highlighting the importance of temperature control in nanoparticle synthesis.

In conclusion, the synthesis of silver nanoparticles using Phyllanthus Niruri leaf extract was successful, producing stable and crystalline nanoparticles. The study demonstrated that pH and temperature play crucial roles in the size,

shape, and rate of nanoparticle formation. The synthesized AgNPs, characterized by various analytical techniques, showed promising properties for potential applications in biomedical and other fields.

### REFERENCES

- [1]. Cademartiri, Ludovico; Ozin, Geoffrey (2009). *Concepts of Nanochemistry*. Germany: Wiley VCH. pp. 4–7. ISBN 978- 3527325979.
- [2]. "Uses of nanoparticles of titanium (IV) oxide (titanium dioxide, TiO<sub>2</sub>)". Doc Brown's Chemistry Revision Notes – Nanochemistry.
- [3]. Wang, Erkang; Wei, Hui (2013-06-21). "Nanomaterials with enzyme like characteristics (nanozymes): next-generation artificial enzymes". *Chemical Society Reviews*. 42 (14): 6060–6093. doi:10.1039/C3CS35486E. ISSN 1460-4744. PMID 23740388
- [4]. Kingshott, Peter. "Electrospun nanofibers as dressings for chronic wound care" (PDF). *Materials Views*. Macromolecular Bioscience.
- [5]. Vert, Michel; Doi, Yoshiharu; Hellwich, Karl-Heinz; Hess, Michael; Hodge, Philip; Kubisa, Przemyslaw; Rinaudo, Marguerite; Schué, François (2012). "Terminology for biorelated polymers and applications (IUPAC Recommendations 2012)" (PDF). *Pure and Applied Chemistry*. 84 (2): 377–410. Doi: 10.1351/PAC-REC-10-12- 04. S2CID 98107080
- [6]. Hussain I, Singh NB, Singh A, et al. Green synthesis of Nanoparticles
- [7]. S. S. Shankar, A. Ahmad, and M. Sastry, "Geranium leaf assisted biosynthesis of silver nanoparticles," *Biotechnology Progress*, vol.19, no. 6, pp. 1627–1631, 2003. View at: Publisher Site | Google Scholar
- [8]. J. L. Gardea-Torresdey, E. Gomez, J. R. Peralta-Videa, J. G. Parsons, H. Troiani, and M. Jose-Yacaman, "Alfalfa sprouts: a natural source for the synthesis of silver nanoparticles," *Langmuir*, vol. 19, no. 4, pp. 1357–1361, 2003. View at: Publisher Site | Google Scholar
- [9]. S. S. Shankar, A. Rai, A. Ahmad, and M. Sastry, "Controlling the optical properties of lemongrass extract synthesized gold nanotriangles and potential application in infrared-absorbing optical coatings," *Chemistry of Materials*, vol. 17, no. 3, pp. 566–572, 2005. View at: Publisher Site | Google Scholar
- [10]. S. P. Chandran, M. Chaudhary, R. Pasricha, A. Ahmad, and M. Sastry, "Synthesis of gold nanotriangles and silver nanoparticles using Aloe vera plant extract," *Biotechnology Progress*, vol. 22, no. 2, pp. 577–583, 2006. View at: Publisher Site | Google Scholar
- [11]. J. Huang, Q. Li, D. Sun et al., "Biosynthesis of silver and gold nanoparticles by novel sundried Cinnamomum camphora leaf," *Nanotechnology*, vol. 18, no. 10, Article ID 105104, 2007. View at: Publisher Site | Google Scholar
- [12]. B. Ankamwar, C. Damle, A. Ahmad, and M. Sastry, "Biosynthesis of gold and silver nanoparticles using Emblicaofficinalis fruit extract, their phase transfer and transmetallation in an organic solution," *Journal of Nanoscience and Nanotechnology*, vol. 5, no. 10, pp. 1665–1671, 2005. View at: Publisher Site | Google Scholar
- [13]. K. B. Narayanan and N. Sakthivel, "Coriander leaf mediated biosynthesis of gold nanoparticles," *Materials Letters*, vol. 62, no. 30, pp. 4588–4590, 2008. View at: Publisher Site | Google Scholar
- [14]. S. Ankanna, T. N. V. K. V. Prasad, E. K. Elumalai, and N. Savithramma, "Production of biogenic silver nanoparticles using Boswellia ovalifoliolata stem bark," *Digest Journal of Nanomaterials and Bio structures*, vol. 5, no. 2, pp. 369–372, 2010. View at: Google Scholar 49
- [15]. P. Rajase kharreddy, P. U. Rani, and B. Sreedhar, "Qualitative assessment of silver and gold nanoparticle synthesis in various plants: a photo biological approach," *Journal of Nanoparticle Research*, vol. 12, no. 5, pp. 1711–1721, 2010. View at: Publisher Site | Google Scholar
- [16]. V. Parashar, R. Parashar, B. Sharma, and A. C. Pandey, "Parthenium leaf extract mediated synthesis of silver nanoparticles: a novel approach towards weed utilization," *Digest Journal of Nanomaterials and Bio structures*, vol. 4, no. 1, pp. 45–50, 2009. View at: Google Scholar
- [17]. *Materials Science and Engineering: C Volume 91, 1 October 2018, Pages 881-*
- [18]. S. H. Lim and S. M. Hudson, *Color. Technol.*, 56, 227 (2004).

- [19]. QL Feng, J Wu, GQ Chen, FZ Cui, TN Kim, JO. Kim *Journal of biomedical materials research*. 52(4), 662 (2000). \* J. R. EJL Morones, A. Camacho, K., Holt J. B. Kouri, J. T. Ramirez, M. J. Yacaman *Nanotechnology*. 16(10), 2346 (2005). \* M. YA Rai, A. Gade, *Biotechnology advances*. 27 (1):76 (2009). \*I. S-SB. Sondi, *Journal of colloid and interface science*. 275 (1):177 (2004).
- [20]. Abdel Rahim, K., Mahmoud, S. Y., Ali, A. M., Almaary, K. S., Mustafa, A. E. Z. M. A. & Husseiny, S. M. (2017). *Extracellular biosynthesis of silver nanoparticles using Rhizopusstolonifer*. *Saudi Journal of Biological Sciences*, 24(1), 208-216.
- [21]. <http://dx.doi.org/10.1016/j.sjbs.2016.02.025> PMID:28053592.
- [22]. Ugwu NI. Sickle cell disease: awareness, knowledge and attitude among undergraduate students of a Nigerian tertiary educational institution. *Asian J Med Sci*. 2016;7(5):87–92. doi:10.3126/ajms.v7i5.15044
- [23]. Onoja SO, Eluke BC, Dangana A, Musa S, Abdullah IN. Evaluation of von Willebrand factor and other coagulation homeostasis profile of patients with sickle cell anemia attending a tertiary hospital at Enugu, Nigeria. *Med J Zambia*. 2020;47(4):269–275. doi:10.55320/mjz.47.4.715
- [24]. Onoja SO, Eluke BC, Dangana A, Musa S, Abdullah IN. Evaluation of von Willebrand factor and other coagulation homeostasis profile of patients with sickle cell anemia attending a tertiary hospital at Enugu, Nigeria. *Med J Zambia*. 2020;47(4):269–275. doi:10.55320/mjz.47.4.7153
- [25]. De Franceschi L, Cappellini MD, Olivieri O. Thrombosis and sickle cell disease. In *Seminars in thrombosis and hemostasis*. *Thieme Med Pub*. 2011;37(3):226–236. doi:10.1055/s-0031-1273087
- [26]. Malowany JJ, Butany J. Pathology of sickle cell disease. *Semin Diagn Pathol*. 2012;29(1):49–55. doi:10.1053/j.semmp.2011.07.005
- [27]. Hsu L, Nnodu OE, Brown BJ, et al. White paper: pathways to progress in newborn screening for sickle cell disease in Sub-Saharan Africa. *J Trop Dis Public Health*. 2018;6(2):260. doi:10.4172/2329-891X.1000260
- [28]. Global Burden of Disease Study. Collaborators (2015). Global, regional, and national incidence, prevalence, and years lived with disability for 301 acute and chronic diseases and injuries in 188 countries, 1990–2013: a systematic analysis for the Global Burden of Disease Study 2013”. *Lancet*. 2013;386(9995):743–800. doi:10.1016/s0140-6736(15)60692-4
- [29]. Rees DC, Williams TN, Gladwin MT. Sickle-cell disease. *Lancet*. 2010;376(9757):2018–2031. doi:10.1016/s0140-6736(10)61029
- [30]. Piel FB, Patil AP, Howes RE, et al. Global epidemiology of sickle haemoglobin in neonates: a contemporary geostatistical model-based map and population estimates. *Lancet*. 2013;381(9861):142–151. doi:10.1016/S0140-6736(12)61229-X
- [31]. Agasa B, Bosunga K, Opara A, et al. Prevalence of sickle cell disease in a northeastern region of the Democratic Republic of Congo: what impact on transfusion policy? *Transfus Med*. 2010;20(1):62–65. doi:10.1111/j.1365-3148.2009.00943.x
- [32]. Afolayan JA, Jolayemi FT. Parental attitude to children with sickle cell disease in selected health facilities in Irepodun Local Government, Kwara State, Nigeria. *Stud Ethno Med*. 2011;5(1):33–40. doi:10.1080/09735070.2011.11886389
- [33]. Kadima BT, Gini Ehungu JL, Ngiyulu RM, Ekulu PM, Aloni MN. High rate of sickle cell anaemia in S ub-Saharan Africa underlines the need to screen all children with severe anaemia for the disease. *Acta Paediatr*. 2015;104(12):1269–1273. doi:10.1111/apa.13040
- [34]. Fleming AF, Storey J, Molineaux L, Iroko EA, Attai ED. Abnormal haemoglobins in the Sudan savanna of Nigeria: i. Prevalence of haemoglobins and relationships between sickle cell trait, malaria and survival. *Ann Trop Med Parasitol*. 1979;73(2):161–172. doi:10.1080/00034983.1979.11687243
- [35]. Galadanci N, Wudil BJ, Balogun TM, et al. Current sickle cell disease management practices in Nigeria. *Int Health*. 2014;6(1):23–28. doi:10.1093/inthealth/iht022.
- [36]. <https://www.easyayurveda.com/2017/05/09/bhumyamalaki-phyllanthus-niruri>.
- [37]. Dhongade H, Chandewar AV. Pharmacognostical, Phytochemical, Pharmacological properties and Toxicological assessment of Phyllanthus amarus. *Interational Journal of Biomedical and Advance Research* 2013; 4(5): NA.

- [38]. [https://www.researchgate.net/publication/358424621\\_Phyllanthus\\_Niruri\\_L\\_A\\_Holistic\\_Medicinal\\_Plant\\_with\\_Modern\\_Therapeutics](https://www.researchgate.net/publication/358424621_Phyllanthus_Niruri_L_A_Holistic_Medicinal_Plant_with_Modern_Therapeutics).
- [39]. Hong-lin, Z. H. U., Wan-xing, W. E. I., Min, Z. H. O. U., Dan, Y. A. N. G., Xi-wang, F. A. N., & Jian-xiong, L. I. U. (2011). Chemical constituents of *Phyllanthus niruri* L. *Natural Product Research & Development*, 23(3).
- [40]. O'Neil J. Maryadle, Annsmith, Heckelman E Patricia, Obenchain R. John Jr., Gallipeau R. Jo Ann, Dárecca Ann Mary: *The Merck Index*. Merck Research Laboratories: New Jersey, 139, 312, 483, 599, 624, 631, 737.
- [41]. Suryanarayana, Challapalli, and M. Grant Norton. *X-ray diffraction: a practical approach*. Springer Science & Business Media, 2013.
- [42]. I. Vamsi Krishna Undavalli, Bhupendra Khandelwal, in *Aviation Fuels*, 2021
- [43]. Stokes, Debbie J. (2008). *Principles and Practice of Variable Pressure Environmental Scanning Electron Microscopy (VP-ESEM)*. Chichester: John Wiley & Sons. ISBN 978-0470758748.
- [44]. Suzuki, E. (2002). "High-resolution scanning electron microscopy of immunogold-labelled cells by the use of thin plasma coating of osmium". *Journal of Microscopy*. 208 (3): 153–157 doi:10.1046/j.1365-2818.2002.01082.x. PMID 12460446. ^ Jump up to: a b c
- [45]. Goldstein, G. I.; Newbury, D. E.; Echlin, P.; Joy, D. C.; Fiori, C.; Lifshin, E. (1981). *Scanning electron microscopy and x-ray microanalysis*. New York: Plenum Press. ISBN 978-0-306-40768-0